Experimental apparatus with full optical access for combustion experiments with laminar flames from a single circular nozzle at elevated pressures

Peter H. Joo, Jinlong Gao, Zhongshan Li, and Marcus Aldén
Division of Combustion Physics, Lund University, P.O. Box 118, S-221 00 Lund, Sweden

(Received 24 September 2014; accepted 9 March 2015; published online 27 March 2015)

The design and features of a high pressure chamber and burner that is suitable for combustion experiments at elevated pressures are presented. The high pressure combustion apparatus utilizes a high pressure burner that is comprised of a chamber burner module and an easily accessible interchangeable burner module to add to its flexibility. The burner is well suited to study both premixed and non-premixed flames. The optical access to the chamber is provided through four viewports for direct visual observations and optical-based diagnostic techniques. Auxiliary features include numerous access ports and electrical connections and as a result, the combustion apparatus is also suitable to work with plasmas and liquid fuels. Images of methane flames at elevated pressures up to 25 atm and preliminary results of optical-based measurements demonstrate the suitability of the high pressure experimental apparatus for combustion experiments. © *2015 AIP Publishing LLC.* [http://dx.doi.org/10.1063/1.4915624]

I. INTRODUCTION

Reciprocating internal combustion engines and jet engines used in ground- and air-based transportation as well as gas-turbines used for power generation all rely on the combustion processes that occur under elevated pressure environments. Considering the reliance on the ubiquitous internal combustion engines and jet engines, as well as gas-turbines, it is important to obtain knowledge-based understanding of the fundamental combustion processes at pressures that are more representative of real conditions. In order to conduct a phenomenological study under elevated pressure environments, e.g., flame temperature structure and species distribution, and understand the physical and chemical processes of combustion, a well-defined premixed and non-premixed flames are necessary to complement and validate the computational modelling efforts. The desirable way to obtain the phenomenological data is to conduct the experiments in a high-pressure combustion apparatus and measure using non-intrusive methods, specifically, optical-diagnostic techniques that can involve the use of many lasers in the setup.

Most high-pressure test rigs, for example, combustor test rigs used in the gas-turbine development are physically large so that it is difficult to move once it is fixed in place. They are also usually complicated to operate that it can require several qualified personnel to operate it safely. Furthermore, due to the relative size of the test section and the geometry of the combustor, it is difficult to maintain a well-defined flame throughout the whole measurement window where a particular combustion phenomenon of interest can be isolated and investigated. Thus, the focus of this work is to report on the design of a high-mobility, laboratory-scale high-pressure combustion apparatus using a novel hybrid design that provides a well-defined flame with full optical access for laser-diagnostic setups.

One of the earliest combustion studies at super-atmospheric pressures was conducted by Burke and Schumann in 1928 with methane-air diffusion flames up to 0.15 MPa and showed that the flame height is independent of pressure if the flows are kept constant.[1] Following the work of Burke and Schumann, still-images of methane-air diffusion flames at pressures up to 5 MPa were presented by Miller and Maahs in a continuous flow high pressure chamber.[2] Additional work with methane was reported by Thomson *et al.* up to 4 MPa and detailed measurements of soot concentrations and temperature profiles in a non-smoking methane-air diffusion flame were reported.[3] The measurements of soot and temperature were later extended to 6.1 MPa by Joo and Gülder[4] and up to 9.1 MPa with methane-oxygen flames.[5] Sooting tendency of ethylene-air diffusion flames was investigated by other investigators using co-flow diffusion flame burners[6–8] and more recently, sooting behaviour of heptane-air flames was examined at pressures up to 0.7 MPa.[9,10] Resonant Coherent anti-Stokes Raman scattering (CARS) spectra of the OH radical have been obtained using a flat flame burner at pressures up to 0.96 MPa[11] and laser-based fluorescence of OH was measured in ethane flames up to 1.25 MPa.[12] Spherically expanding premixed flames of hydrogen-propane-air were investigated up to 0.5 MPa[13] and counter-flow diffusion flames up to 2 MPa were examined and flame structures and extinction conditions of methane, ethane, and ethylene were reported.[14]

The high pressure experimental devices employed by the previous investigators to study the high pressure flames are containment-based chambers[2,5,8,11,12,14] in that a burner can be placed wholly in the chamber, whereas, in the system used by Zhou *et al.*,[10] a burner is partially inserted and sealed in one of the large ports in the chamber so that when the chamber is pressurized, the inserted portion of the burner is exposed to high pressure while the remaining portion is open to the ambient laboratory conditions. This type of high pressure

0034-6748/2015/86(3)/035115/7/$30.00

chamber-burner design is advantageous where space is limited because the device can be relatively small compared to the containment-based high pressure chambers and the burner is easily accessible. For the containment-based chambers, there must be sufficient space in the chamber to fit a whole burner and the access to the burner often requires heavy machinery to handle the large chamber.

A hybrid-type experimental combustion apparatus that is suitable to study flames at pressures up to 3.5 MPa with full optical access was designed and developed. The novelty of this design is that a part of the high-pressure chamber functions as an integral part of the burner. The rest of the burner components are attached and sealed inside the chamber. This is in contrast to the designs used by previous investigators in that it is neither a wholly containment-based nor chamber-burner combustion chamber. The versatility of this hybrid-type high pressure combustion apparatus is that the burner is easily accessible without heavy machinery and the chamber is relatively large to enable different burner configurations or use other burner types, but small enough that it can easily be moved to different laboratory rooms for measurements. In this work, we report on the design of the hybrid-type high pressure combustion apparatus and give some representative results by providing still-images and optical-based measurements of laminar flames at high pressure to demonstrate the functionality of the burner and the optical accessibility of the apparatus.

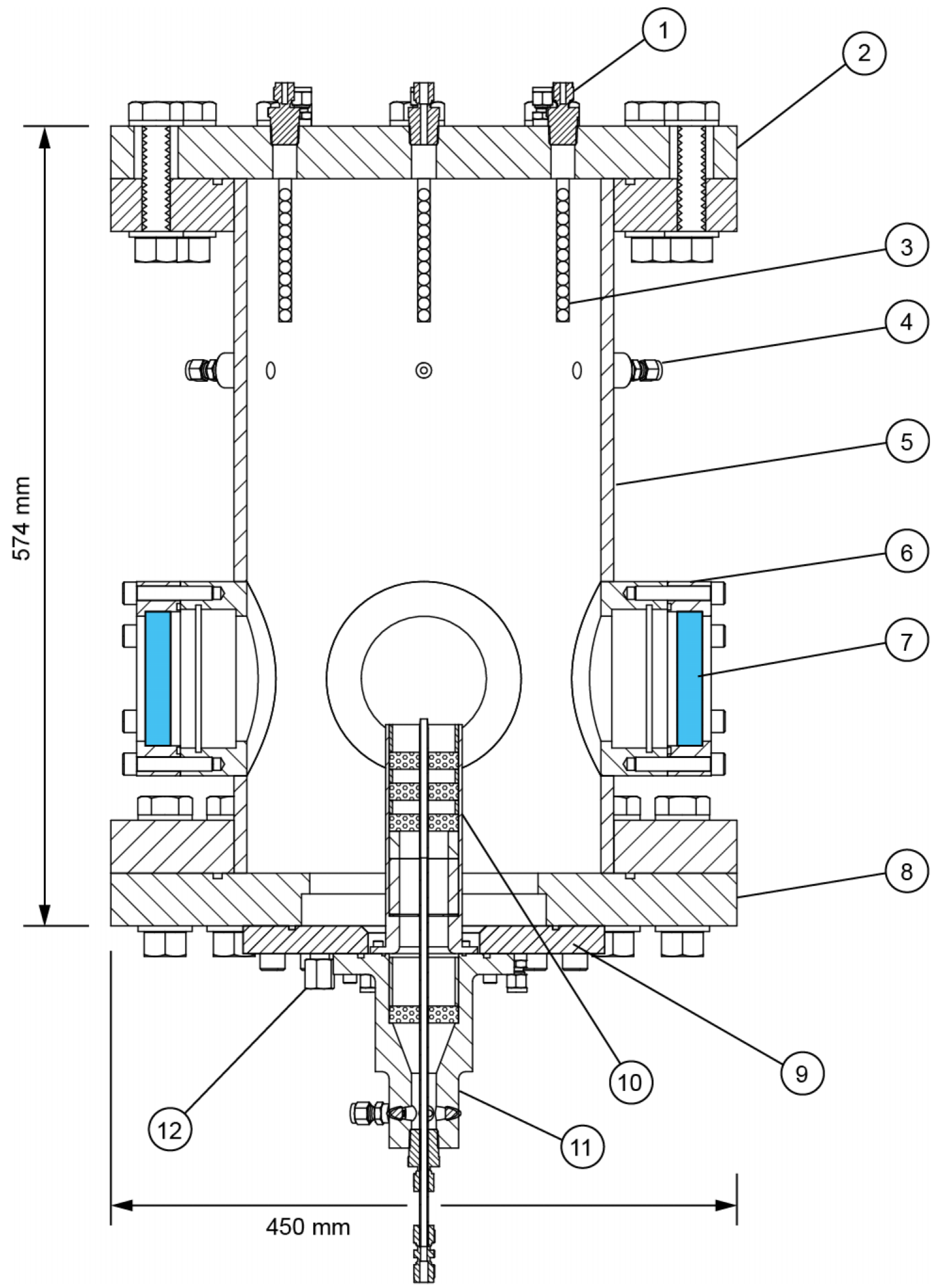

FIG. 1. General schematics of the high pressure combustion apparatus. 1—Access ports. 2—Top cap flange. 3—Cooling coils in series. 4—Access ports. 5—Chamber tube. 6—Window frames. 7—Anti-reflection coated sapphire windows. 8—Bottom cap flange. 9—Mounting plate. 10—Interchangeable burner module. 11—Chamber burner module. 12—Access ports.

II. HIGH PRESSURE APPARATUS

A. High-pressure chamber and burner

The general schematic of the high pressure combustion apparatus is provided in Fig. 1. The high-pressure combustion apparatus is constructed using stainless-steel for superior material compatibility with many fluids. The chamber is rated for maximum pressure of 3.6 MPa and maximum temperature of 220 °C. The internal volume of the chamber is 25 litres. The height of the chamber between the cap flanges is 574 mm and the width is 450 mm. The inner diameter of the chamber tube (item 5, Fig. 1) is 254.5 mm, the height is 500 mm, and the thickness is 9.2 mm. Standard flanges are used and are welded onto the tube, except for the cap flanges where the seal is obtained using standard o-rings. The high pressure chamber has four viewports positioned at angles 0°, 90°, 180°, and 270° for full optical access into the chamber for various line-of-sight and scattering optical diagnostic techniques. The high pressure chamber is equipped with six access ports on the chamber tube (item 5, Fig. 1), eight on the top flange (item 2, Fig. 1), and eight on the mounting plate (item 9, Fig. 1) with six M6 attachment threads to utilize pass-through connection systems and mount electro-mechanical devices in the chamber. The electrical pass-through connections are obtained using Conax connectors. The high pressure chamber is fitted with three rupture discs and two relief valves to mitigate over-pressurization. Also, as a precautionary safety measure, thermocouples (k-type) are inserted into the chamber to monitor the temperature at various locations.

The high pressure burner is comprised of two modules. The first module is the Interchangeable Burner Module (IBM, item 10, Fig. 1) and the second module is the Chamber Burner Module (CBM, item 11, Fig. 1). An exploded view of the burner module assembly is provided in Fig. 2 and a representative picture of the assembled burner is provided in Fig. 3. The chamber module of the burner acts as a common base for the interchangeable burner module and it is an integral part of the chamber that is bolted onto the mounting plate (item 9, Fig. 1). The IBM is independent of the chamber and it resides wholly in the chamber. This hybrid chamber-burner design permits the use of different IBM(s) by using the common CBM and therefore, there is no need to make changes to the structure of the chamber. Thus, a relatively compact chamber with a burner that is easily accessible but still large enough to accommodate different types of burners can be constructed without affecting the original safety compliance every time a new burner is installed.

The assembly of the IBM and the CBM make a normal co-flow burner with a long tube in the center that carries the combustible gas and acts as a flame anchor. The outside diameter of the central burner tube can be as large as 12 mm. The burner is comprised of flow settling sections where a series of porous metal cylinders are used to remove the instabilities in the flow and provide a uniform flow at the exit. The porous metal cylinders are positioned by stainless-steel spacers of various lengths and thus the configuration can be altered readily. The IBM can be accessed easily by either removing the mounting plate (item 9, Fig. 1) or removing the

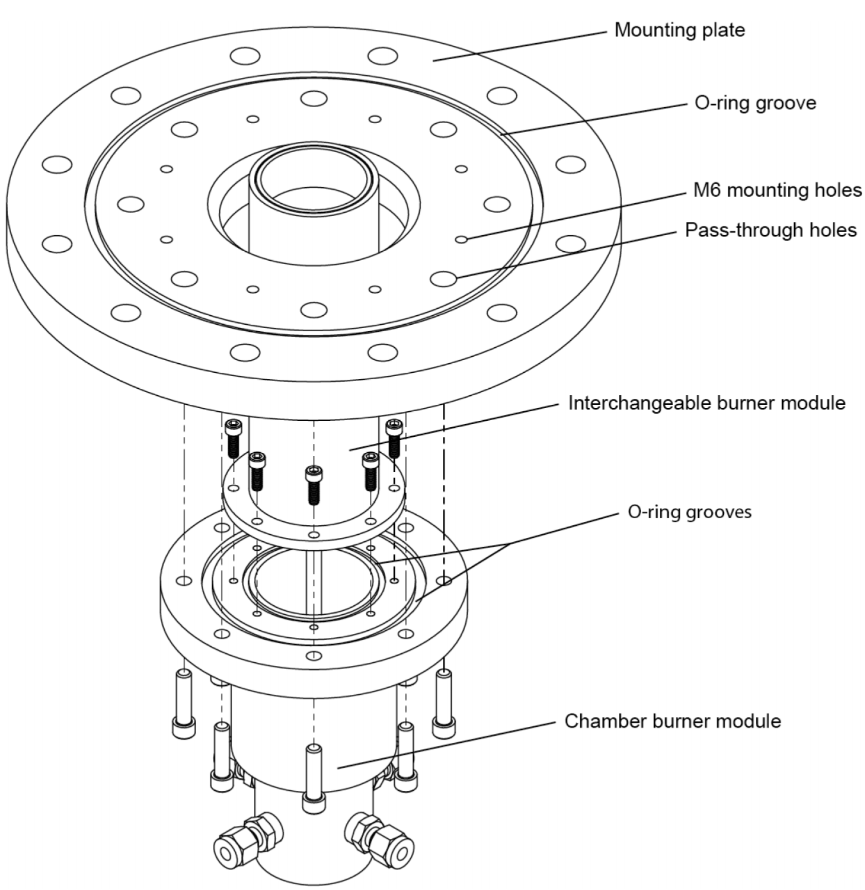

FIG. 2. An exploded view of the burner assembly modules with the mounting plate.

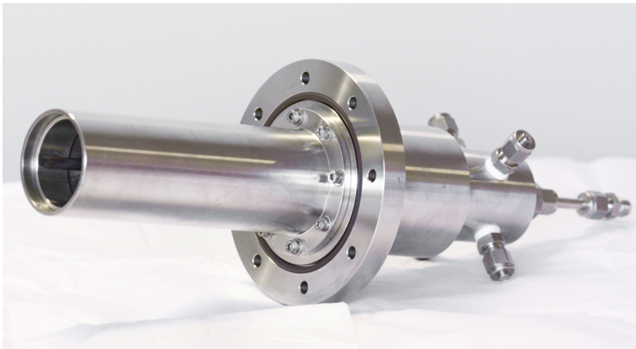

FIG. 3. A representative picture of the high pressure burner. Shown are the Interchangeable Burner Module (IBM) and the Chamber Burner Module (CBM).

chamber burner module (item 11, Fig. 1) without removing any of the chamber cap flanges.

B. Pressure and flow control

The pressure in the chamber is created by the continuous flow of gases into the chamber from the high pressure gas cylinders stored in safety cabinets and controlled by regulating the flow of gases as they exit the chamber using electronic and manually operated back-pressure regulators. The back-pressure regulators are connected downstream of the exhaust line so that the gases are cooled in the line as they flow to the regulators. During the operation, the chamber pressure deviates less than 1% from the setpoint. The flow rates of gases into the chamber can be controlled with manually operated by-pass valves and with thermal-based high pressure mass flow controllers (MFCs) that are tethered to a computer control station. Each mass flow controller is connected to a dedicated forward-pressure regulator and where higher flow rates are needed, additional mass flow controllers are connected in parallel to the dedicated forward-pressure regulator to increase the total flow rate. The pressure and the flow rates are monitored continuously and controlled at the computer control station that is located behind a Lexan safety shield to protect the laboratory personnel should the equipment fail.

C. High temperature

The chamber contains numerous access ports for thermocouple inputs and electrical pass-through connections. These access ports are used with Conax connectors to transmit electrical signals for feedback control to conduct experiments with liquid fuels as well as experiments involving plasma at elevated

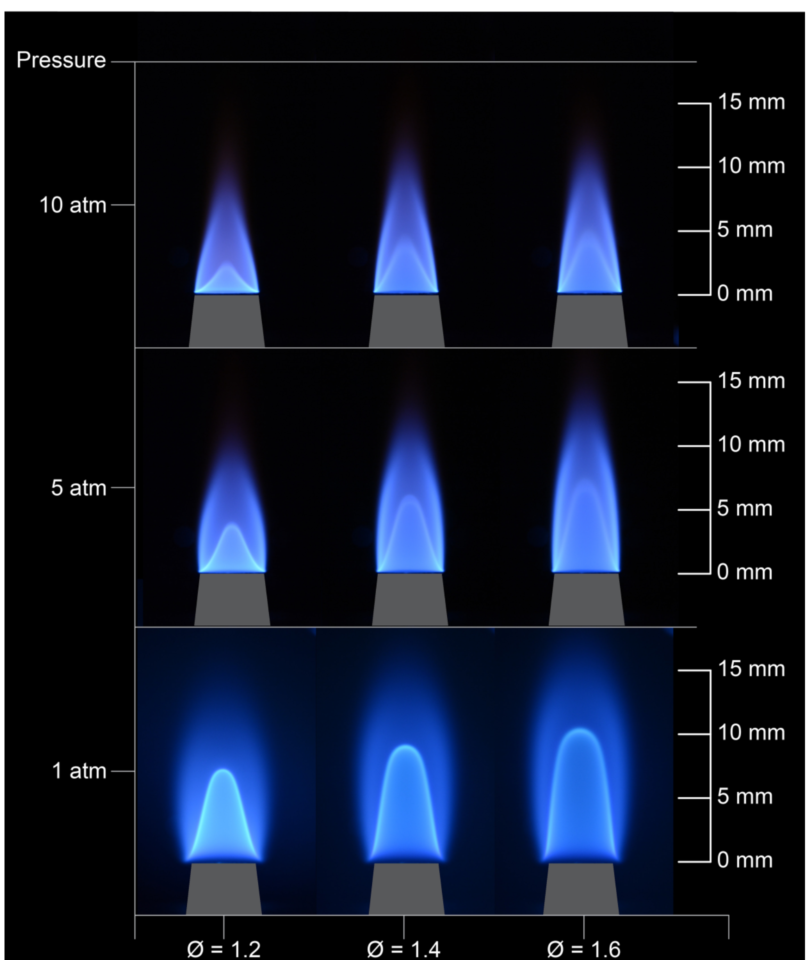

FIG. 4. Premixed methane-air flames from a conical nozzle up to 10 atm. The pressure is fixed for each of the equivalence ratios (along the rows). The mass flow rate of methane is fixed at 1.11 mg/s for all of the cases. The inside diameter of the conical nozzle is 5 mm. The light exposure setting on the camera is fixed for all of the cases to maintain consistency.

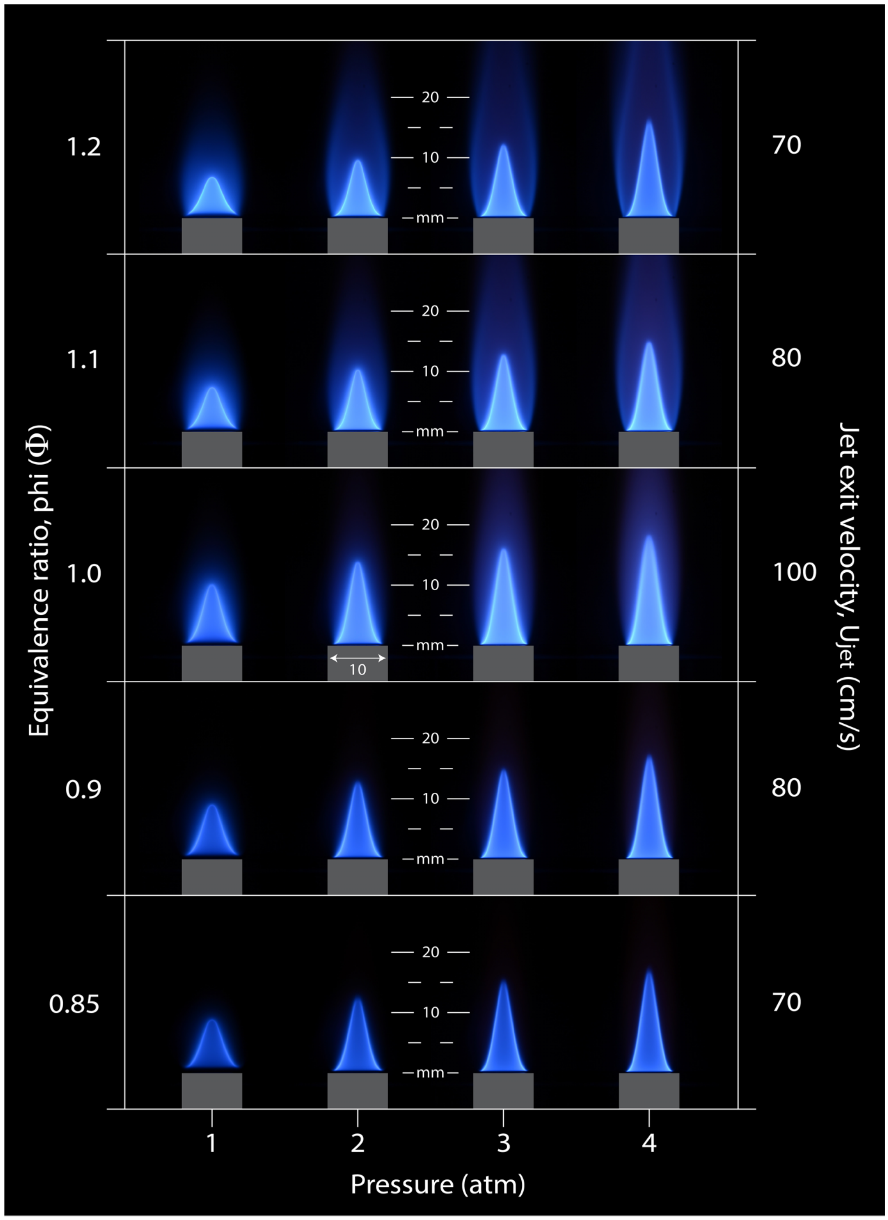

FIG. 5. Premixed methane-air flames from a circular nozzle up to 4 atm. The inside and outside diameter of the nozzle are 7 and 10 mm, respectively. The jet exit velocities are fixed for each of the given equivalence ratios. The light exposure setting on the camera is fixed for all of the cases to maintain consistency.

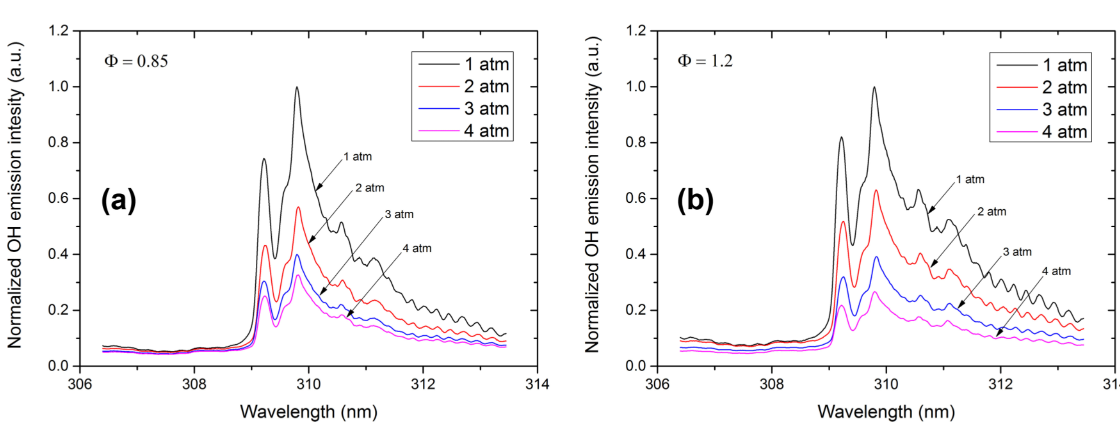

FIG. 6. Spectral measurements of normalized OH chemiluminescence intensity centered at 310 nm from a methane-air flame for pressures between 1 and 4 atm. The spectral intensity data are divided by the mass flow rate at each pressure, then normalized by the highest measured value. (a) Lean phi = 0.85, (b) Rich phi = 1.2 methane-air flame.

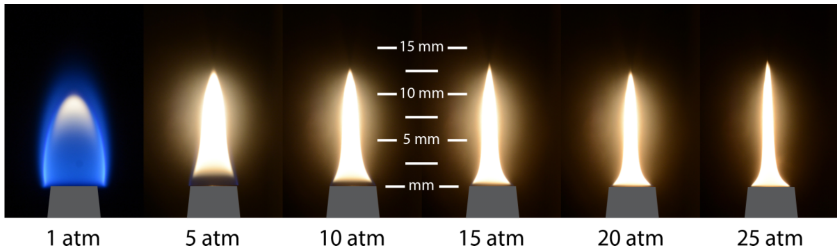

FIG. 7. Methane-air diffusion flames from a conical nozzle. The inside diameter of the nozzle is 5 mm and the methane mass flow rate is fixed at 0.83 mg/s for all of the cases. The light exposure setting on the camera is adjusted to prevent over-saturation.

pressures. To vaporize liquid fuels and to ensure no condensation occurs in the fuel line carrying the vaporized liquid fuel, the burner can be heated up to 220 °C using controlled electrical heating devices both inside and outside the chamber.

D. Optical access

The optical access to the burner is provided through sapphire windows on the chamber viewports. The sapphire windows have an anti-reflection coating at wavelengths from 250 to 430 nm and at 560 nm. The thickness of the windows is 18 mm and the viewable diameter is 90 mm. The sapphire windows are sealed onto a stainless-steel housing frame with a bolt-hole pattern so that these windows can be mounted easily onto the viewports with the matching bolt-hole pattern on the chamber. A standard o-ring is used between the sapphire window housing frame and the chamber viewport to obtain the seal.

E. Temperature control and vapor condensation

The high pressure chamber is equipped with multiple cooling coils in series to help moderate the temperature in the chamber. The cooling fluid can be normal water for simplicity but other fluids can be used as well. The cooling coils also act as a water vapor condenser because the cold surfaces of the cooling coils are an attractive surface for the vapor to condense to liquid water. The viewport windows on the chamber are wrapped with PID controlled heating bands to remove any water vapor condensation should it condense on the windows. Furthermore, air or a diluent gas can be introduced through the chamber ports to reduce the temperature and evacuate the gases, should the chamber needs to be purged.

F. Ignition

The fuel or the flammable mixture flowing from the burner nozzle can be ignited using a resistive heating coil or a ceramic glow-stick that is positioned directly above the burner. The igniter is attached to a linear translation device so that once the combustible mixture is ignited, the power to the igniter is cut and the igniter is translated vertically out of the flame flow field. Thus, a high pressure flame is obtained with the following procedure: (1) the chamber is fully closed so as to pressurize the chamber from the atmospheric conditions; (2) the igniter is turned on and the combustible mixture flows through the burner; (3) once the mixture is ignited, the igniter is turned off and translated vertically away from the flame; (4) the back-pressure regulators are adjusted until the desired pressure is reached.

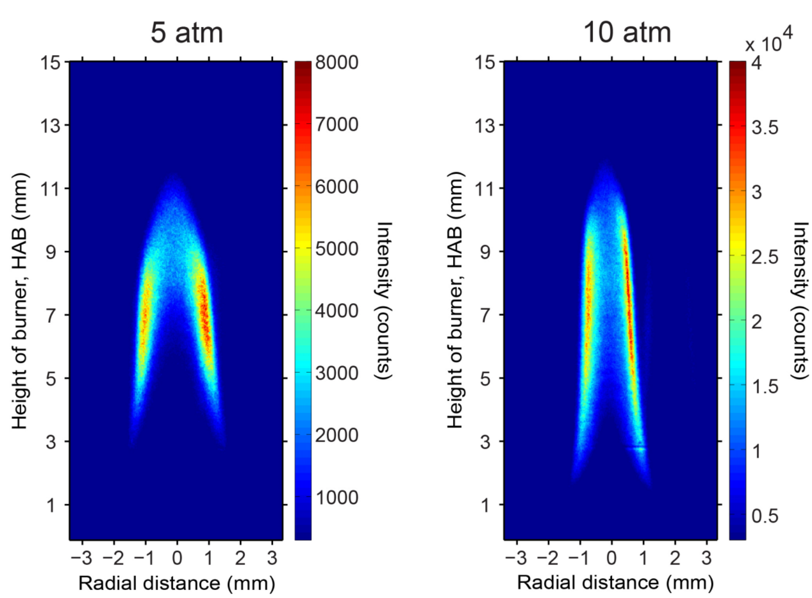

FIG. 8. Representative laser-induced incandescence images of sooting methane-air diffusion flames at pressures 5 and 10 atm. Methane mass flow rate is fixed at 0.83 mg/s for both of the cases.

III. OPTICAL MEASUREMENTS

Representative still-images of rich methane-air flames anchored on a 5 mm inside diameter conical nozzle at pressures up to 10 atm are provided in Fig. 4. For the flames in Fig. 4, the mass flow rate of the fuel is fixed at 1.11 mg/s for all of the cases. At atmospheric pressure, a typical Bunsen-type premixed flame is represented well with the reaction and production zones that are visibly distinct. As the pressure increases, the overall size of the visible flame appears to get smaller and the flame becomes conical.

Still-images of lean and rich premixed methane-air flames anchored on a slightly larger nozzle, 7 mm inside diameter, at pressures up to 4 atm are provided in Fig. 5. For the flames in Fig. 5, the jet exit velocities are fixed for each of the given equivalence ratios. Thus, the mass flow rate of the combustible mixture increases with pressure, given a fixed equivalence ratio and jet exit velocity. It appears that the overall size of the visible flame increases with pressure regardless of the equivalence ratio if the jet exit velocity is kept constant. The spectral measurements of OH chemiluminescence with center wavelength at 310 nm and at the equivalence ratio of 0.85 for the pressures between 1 and 4 atm are provided in Fig. 6(a). The intensities are binned over the whole flame from the tip of the nozzle to the tip of the inner flame cone based on visual inspection. Then, the emission intensities are divided by the mixture mass flow rates for each of the pressures and normalized by the highest measured value, that is, the highest intensity obtained at the equivalence ratio of 0.85 and 1 atm. The same method was applied to the rich methane flame at the equivalence ratio of 1.2 and the OH chemiluminescence measurements are provided in Fig. 6(b). For the lean flames, our work agrees well with other investigators that the OH chemiluminescence has an inverse dependence on pressure.[15] In both lean and rich flames, it appears that the OH chemiluminescence emission intensities decrease monotonically with increasing pressures.

Still-images depicting highly sooting methane-air diffusion flames at elevated pressures are provided in Fig. 7. At atmospheric pressure, the flame is bulbous and the visible sooting zone is located near the flame tip. As the pressure increases, however, the sooting zone moves towards the burner tip and at 25 atm, the flame appears to be completely yellow and slender. Furthermore, laser-induced incandescence measurements were conducted using a pulsed, frequency doubled 532 nm Nd:YAG laser. The laser energy was kept at 220 mJ and the height of the laser sheet at approximately 2 cm. Representative single-shot images of laser-induced incandescence (LII) of sooting diffusion flames at pressures 5 and 10 atm are provided in Fig. 8. At atmospheric pressure, the LII signal was too weak to record any images. However, as the pressure increases, soot concentrations increase significantly and it appears that the location of the peak concentrations is near the mid-height of the flame. The sooting observations are in agreement with other work at high pressure[4,5] and this provides additional support to the experimental apparatus to conduct combustion experiments at elevated pressures.

ACKNOWLEDGMENTS

We thank the Swedish Energy Agency through the Centre of Combustion Science and Technology (CECOST), the Knut & Alice Wallenberg foundation, Swedish-China collaboration project (Project No. 33305-1), the European Research Council (ERC) Advanced Grant through DALDECS program, and the Swedish Research Council (VR) for their generous support.

[1]S. P. Burke and T. E. W. Schumann, Ind. Eng. Chem. **20**, 998–1004 (1928).
[2]I. M. Miller and H. G. Maahs, NASA Technical Note TN D-8407, 1977.
[3]K. A. Thomson, Ö. L. Gülder, E. J. Weckman, R. A. Fraser, G. J. Smallwood, and D. R. Snelling, Combust. Flame **140**, 222–232 (2005).
[4]H. I. Joo and Ö. L. Gülder, Proc. Combust. Inst. **32**, 769–775 (2009).
[5]H. I. Joo and Ö. L. Gülder, Combust. Flame **157**, 1194–1201 (2010).
[6]W. L. Flower, Combust. Flame **77**, 279–293 (1989).
[7]H. I. Joo and Ö. L. Gülder, Combust. Flame **158**, 416–422 (2011).
[8]L. L. McCrain and W. L. Roberts, Combust. Flame **140**, 60–69 (2005).
[9]A. E. Karatas, G. Intasopa, and Ö. L. Gülder, Combust. Flame **160**, 1650–1656 (2013).
[10]L. Zhou, N. J. Dam, M. D. Boot, and L. P. H. de Goey, Combust. Flame **160**, 2507–2516 (2013).
[11]B. Attal-Tretout, S. Schmidt, E. Crete, P. Dumas, and J. Taran, J. Quant. Spectrosc. Radiat. Transfer **43**, 351–364 (1990).
[12]C. D. Carter, G. B. King, and N. M. Laurendeau, Appl. Opt. **31**, 1511–1522 (1992).
[13]C. Law, G. Jomaas, and J. Bechtold, Proc. Combust. Inst. **30**, 159–167 (2005).
[14]U. Niemann, K. Seshadri, and F. A. Williams, Combust. Flame **161**, 138–146 (2014).
[15]B. Higgins, M. McQuay, F. Lacas, J. Rolon, N. Darabiha, and S. Candel, Fuel **80**, 67–74 (2001).